

Magnetic phase transitions and the magnetothermal properties of gadolinium

S. Yu. Dan'kov and A. M. Tishin

Physics Department, M. V. Lomonosov Moscow State University, Moscow, 119899, Russia

V. K. Pecharsky* and K. A. Gschneidner, Jr.

Ames Laboratory and Department of Materials Science and Engineering, Iowa State University, Ames, Iowa 50011-3020

(Received 5 September 1997)

A study of four Gd samples of different purities using ac susceptibility, magnetization, heat capacity, and direct measurements of the magnetocaloric effect in quasistatic and pulse magnetic fields revealed that all techniques yield the same value of the zero-field Curie temperature of 294(1) K. The Curie temperature determined from inflection points of the experimental magnetic susceptibility and heat capacity is in excellent agreement with those obtained from the magnetocaloric effect and Arrot plots. Above 2 T the temperature of this transition increases almost linearly with the magnetic field at a rate of ~ 6 K/T in fields up to 7.5 T. The spin reorientation transition, which occurs at 227(2) K in the absence of a magnetic field, has been confirmed by susceptibility, magnetization, and heat-capacity measurements. Magnetic fields higher than 2–2.5 T apparently quench the spin reorientation transition and Gd retains its simple ferromagnetic structure from the $T_C(H)$ down to ~ 4 K. The nature of anomaly at $T \cong 132$ K, which is apparent from ac susceptibility measurements along the c axis, is discussed. The presence of large amounts of interstitial impurities lowers the second-order paramagnetic \leftrightarrow ferromagnetic transition temperature, and can cause some erroneous results in the magnetocaloric effect determined in pulsed magnetic fields. The magnetocaloric effect was studied utilizing the same samples by three experimental techniques: direct measurements of the adiabatic temperature rise, magnetization, and heat capacity. All three techniques, with one exception, yield the same results within the limits of experimental error. [S0163-1829(98)01606-3]

I. INTRODUCTION

Gadolinium is the only rare earth which orders magnetically near room temperature and is often considered to be a simple Heisenberg ferromagnet, i.e., a representative classical ferromagnet. The paramagnetic \leftrightarrow ferromagnetic phase transition is a second-order phase transformation. The magnetic moment of Gd is quite large and is due to the presence of seven unpaired $4f$ electrons which have a total angular momentum of $J=L+S=7/2$. Gd crystallizes in the hexagonal close-packed structure.

The magnetic properties of Gd metal have been extensively studied.¹ According to neutron-diffraction studies, it orders ferromagnetically below the Curie point, $T_C \cong 293$ K, and remains ferromagnetic down to liquid-helium temperatures.² The easy magnetization axis coincides with the crystallographic sixfold symmetry axis, i.e., the [0001] direction in the crystal lattice, from T_C down to the spin reorientation temperature, $T_{SR} \cong 230$ K. Below T_{SR} , the easy magnetization vector departs from the [0001] direction, and the cone angle between the sixfold symmetry axis and the easy magnetization axis changes with temperature.

The magnetic and thermal properties of Gd continue to attract attention even at the present time. First, the phase transitions in Gd are enticing from a theoretical standpoint. In particular, it is known that the magnetic phase transitions in some heavy lanthanide metals have coexisting features of first-order and second-order phase transformations.³ Since Gd is considered a classical ferromagnet and it orders near room temperature, it is quite easy to carry out experiments to gain a better understanding of the nature of the

paramagnetic \leftrightarrow ferromagnetic phase transformation. Second, this transformation has a potentially large practical importance, specifically with regard to magnetic cooling and heating near room temperature. It is well known that the heating and cooling of a magnetic material (i.e., the magnetocaloric effect) is the largest near T_C . This occurs because the two opposite forces (the ordering force due to exchange interaction of the magnetic moments, and the disordering force of the lattice thermal vibrations) are approximately balanced near the T_C . Hence, the isothermal application of a magnetic field produces a much greater increase in the magnetization (i.e., an increase of the magnetic order and, consequently, a decrease in magnetic entropy, ΔS_{mag}) near the Curie point, rather than far away from T_C . The effect of magnetic field above and below T_C is significantly reduced because only the paramagnetic response of the magnetic lattice can be achieved for $T \gg T_C$, and for $T \ll T_C$ the spontaneous magnetization is already close to saturation and cannot be increased much more. Similarly, the adiabatic (isentropic) application of a magnetic field leads to an increase in the magnetic material temperature, ΔT_{ad} , which is also sharply peaked near the T_C . Therefore, a detailed experimental study of the magnetic and thermal properties of Gd are quite important.

Reports on the magnetic properties of single crystalline Gd can be found in many publications (for example, see Refs. 4–10). They include detailed studies of the magnetization and susceptibility near the Curie point,⁵ the anisotropy of the susceptibility near T_C ,⁶ the magnetic moment along different crystallographic directions from 1.4 to 300 K in applied fields up to 2 T,⁷ and the magnetization from 80 to 360 K in pulse fields up to 30 T.⁸ However, as noted in Ref.

TABLE I. The effect of the experimental technique and purity on the Curie temperature of Gd from a selected list of publications.

Experimental technique	T_C (K)	Purity	Reference
Magnetization	292	Unknown	4
	290 ± 1	99.9 wt. %	19
	289 ± 2	99.9 wt. %	20
Magnetic susceptibility	293 ± 1	Unknown	5
	290	99.9 wt. %	21
Neutron scattering	291	99.9 wt. %	22
Magnetocaloric effect	295	99.99 wt. %	15
	293	Unknown	24
	292.25	99.99 wt. %	25
Photoemission	290	Unknown	23
Heat capacity	293	99.4 wt. %	16
	293.5	Unknown	17
	292.2	99.9 wt. %	18

10, the magnetic properties of Gd and other lanthanides are critically dependent on their purity, and unfortunately most of the studies mentioned above were performed on different (in terms of the amount of various impurities) specimens. In many cases the impurity content was unknown. Furthermore, the exact constitution of the Gd magnetic H - T diagram is still unclear. A total of four anomalies of the magnetic susceptibility of single crystalline Gd in zero field were noted in Ref. 3. Two of them are located near the T_C , a third near T_{SR} , and a fourth near 140 K. The magnitude of these anomalies is reduced upon the application of magnetic fields. The anomalies on the temperature dependence of Young's modulus³ and the anisotropy constant K_1 ,¹¹ were also reported near 140 K.

The heat capacity is a useful tool for studying magnetic phase transitions in the lanthanide metals and their compounds. Theoretical and experimental investigations of the heat-capacity behavior of some Gd-based compounds can be found in the literature, e.g., see Refs. 12–14. Usually the heat capacity at constant pressure $C_p(T)$ behaves abnormally near the temperature where magnetic phase transitions occur. Hence, the behavior of $C_p(T, H)$ as a function of temperature and magnetic field can be used to examine the nature of the magnetic phase transition. Furthermore, the experimental $C_p(H, T)$ data allow one to calculate the magnetocaloric effect (MCE).¹⁵ As far as we are aware the heat capacity in the vicinity of paramagnetic \leftrightarrow ferromagnetic phase transition in polycrystalline Gd was measured from 15 to 355 K,¹⁶ and on single-crystal samples from 200 to 330 K (Ref. 17) and from ~ 275 to ~ 315 K.¹⁸ No reports on the experimentally measured heat capacity of Gd in magnetic fields, except at very low fields of 39–139 mT,¹⁸ is available in the literature, although the MCE results calculated from $C_p(H, T)$ have been reported.¹⁵

One of the important characteristics of the magnetic phase transition is the exact ordering temperature. However, as can be seen from published data, the evolution of the Curie temperature in Gd seems to be sensibly dependent on the experimental technique, the magnetic and thermal history of the sample, and its purity. This is illustrated in Table I where the values of the Curie temperature of Gd are listed in six dif-

ferent groups according to the experimental techniques used in the various studies. The spread of reported Curie temperature varies from 289 to 295 K. Hence, the question about the extent to which different experimental measurements and the degree of purity of the metal alters the deduced result remains open.

In this paper we report on a variety of experimental measurements (including ac and dc magnetic susceptibility, dc magnetization, zero field and dc magnetic-field heat capacity, and direct magnetocaloric measurements in quasistatic and pulsed magnetic fields) performed on several different Gd samples. The resultant experimental data have been used for detailed analysis of magnetic phase transitions in Gd and to refine its H - T magnetic phase diagram. Also the magnetocaloric effect (MCE) was calculated from: (1) both the magnetization and the magnetic heat capacity as the isothermal magnetic entropy change, $\Delta S_{\text{mag}}(T)$; and (2) from the magnetic heat capacity as the adiabatic temperature rise, $\Delta T_{\text{ad}}(T)$. In addition $\Delta T_{\text{ad}}(T)$ was measured directly. Both $\Delta S_{\text{mag}}(T)$ and $\Delta T_{\text{ad}}(T)$ were calculated and/or measured as a function of temperature for several fixed magnetic field changes from 0 to H , where $\mu_0 H$ varied from ~ 0.5 to 10 T.

II. EXPERIMENTAL TECHNIQUES

The magnetocaloric effect ΔT_{ad} was measured from ~ 77 to 350 K in both quasistatic and pulsed fields. The magnetic field for the quasistatic measurements ranged from 0 to 2 T and was created by an electromagnet. Due to the relatively large magnetic induction, the time of a field sweep from 0 to 2 T was $\tau \cong 2$ s. The measurements were made on a thermally insulated (in a vacuum of $\sim 10^{-3}$ Torr) sample to minimize heat exchange between the specimen and the surroundings. The equilibrium temperature of the specimen was measured using copper-constantan thermocouple before and after the field sweep. The magnetocaloric effect was determined as the difference between the two equilibrium temperatures. A detailed description of the 0–7 T pulsed field apparatus and the measurement procedure has been published elsewhere.²⁶ The experimental errors for the two direct measurement techniques were estimated to be $\sim 7\%$ for each.²⁶

The heat capacity in zero magnetic field and in magnetic fields 2, 5, 7.5, and 10 T was measured from ~ 3.5 to 350 K by using a heat-pulse calorimeter which has been described elsewhere.²⁷ The accuracy of heat-capacity data was $\sim 1\%$ in the temperature range from 3.5 to ~ 20 K, and less than $\sim 0.5\%$ in the temperature range from 20 to 350 K. The measured heat-capacity data, $C_p(T, H_i)$, (typically a total of ~ 300 data points for each magnetic field) were used to calculate the total entropy, $S_{\text{total}}(T, H_i)$ where H_i is a fixed magnetic field, $\mu_0 H = 0, 2, 5, 7.5,$ or 10 T. It is well known that the total entropy as a function of temperature is given as

$$S_{\text{total}}(T, H_i) = \int_0^T \frac{C_p(T, H_i)}{T} dT + S_0(H_i). \quad (1)$$

Here $S_0(H_i)$ is the integration constant which is assumed to be field independent and equal to 0. To minimize the effect of a varying starting temperature during the heat-capacity measurements in different magnetic fields, a numerical inte-

gration was always performed beginning at a common lowest temperature T_{\min} for all fields. Thus, the entropy was calculated as follows:

$$S_{\text{total}}(T, H_i) = \int_0^{T_{\min}} \frac{C'_p(T, H_i)}{T} dT + \int_{T_{\min}}^T \frac{C_p(T, H_i)}{T} dT. \quad (2)$$

Here $C'_p(T, H_i)$ of the first term on the right-hand side of Eq. (2) was extrapolated from $T = T_{\min}$ to $T = 0$ K using the experimental data measured between ~ 3.5 and ~ 8 K and assuming that the total heat capacity is the sum of the electronic, lattice and magnetic contributions: $C_{\text{total}} = C_{\text{el}} + C_{\text{lat}} + C_{\text{mag}}$. For pure Gd: the electronic heat capacity, $C_{\text{el}} = \gamma T$, with $\gamma = 4.48$ mJ/mol K²; the lattice heat capacity, $C_{\text{lat}} = \beta T^3$, where β is a function of the Debye temperature, $\Theta_D = 169$ K; and the magnetic heat capacity, $C_{\text{mag}} = BT^n$, with $B = 1.37$ mJ/mol K^{2.5}, and $n = 1.5$ for zero magnetic field.²⁸ During the extrapolation we assumed that electronic (γ) and lattice (β) heat-capacity constants are independent of the magnetic field and that the magnetic field only affects the magnetic heat-capacity constant B . Therefore, the value of B was the only parameter determined from a least-squares fit of higher temperature heat-capacity data (T_{\min} to ~ 8 K) and then used in interpolation of the heat-capacity data from $T = T_{\min}$ to $T = 0$ K.

Assuming that the errors in temperature measurements are negligible compared to the errors in heat capacity, $\sigma C_p(T, H_i)$, the errors in total entropy, $\sigma S(T, H_i)$, can be estimated from Eq. (2):

$$\sigma S(T, H_i) = \int_0^{T_{\min}} \frac{\sigma C'_p(T, H_i)}{T} dT + \int_{T_{\min}}^T \frac{\sigma C_p(T, H_i)}{T} dT. \quad (3)$$

Hence, the errors in the entropy are also of the order of $\sim 1\%$ in the temperature range from 3.5 to ~ 20 K and less than 1% of $S_{\text{total}}(T, H_i)$ at higher temperatures.

The magnetic entropy change for a magnetic field change from 0 to H_i was calculated from the heat-capacity data as the isothermal difference, and the adiabatic temperature rise was calculated as the adiabatic (isentropic) difference between $S_{\text{total}}(T, 0)$ and $S_{\text{total}}(T, H_i)$. According to Ref. 15, the corresponding errors $\sigma \Delta S_{\text{mag}}$ and $\sigma \Delta T_{\text{ad}}$ are

$$\sigma \Delta S_{\text{mag}}(T) = \sigma S(T, 0) + \sigma S(T, H_i) \quad (4)$$

and

$$\sigma \Delta T_{\text{ad}}(T) = \sigma S(T, 0) \left/ \left(\frac{dS(T, 0)}{dT} \right) \right. + \sigma S(T, H_i) \left/ \left(\frac{dS(T, H_i)}{dT} \right) \right. \quad (5)$$

The ac and dc magnetic susceptibility and the dc magnetization were measured using a commercial ac/dc susceptometer/magnetometer, model 7225, manufactured by the Lake Shore Cryotronics, Inc. The magnetic measurements were made in the temperature range from 4.5 to 325 K in dc fields from 0 to 5.6 T. The ac fields ranged from 0.25 to 1 mT (2.5 to 10 Oe) and the ac field frequencies varied from

TABLE II. The chemical analysis for the Gd metal samples used in this study. The impurity contents are listed as ppm atomic. A dash indicates that the impurity level was < 1 ppm atomic.

Impurity	Sample 1 Gd-M1 polycrystal	Sample 2 MPC, polycrystal	Sample 3 MPC, single crystal	Sample 4 China polycrystal
H	31 540	155	63	32 300
C	2480	196	470	10 480
N	3190	90	100	4490
O	32 511	442	706	11 840
F	130	25	20	8270
Al	270	2	11	21
Si	1200	2	25	92
Cl	1300	-	12	2
Ca	-	-	-	1000
Fe	340	36	27	170
Ni	87	3	8	25
Cu	390	2	25	450
Zn	2	-	15	-
Y	170	-	-	11
Dy	77	-	-	19
Lu	30	-	-	55
Ta	-	-	-	170
W	-	3	5	-
Overall purity, at.%	92.63	99.90	99.85	93.06
Overall purity, wt.%	99.49	99.99	99.98	99.68

55 to 1000 Hz. The accuracy of magnetic measurements cannot be easily estimated since no corresponding data are specified by the manufacturer, however, measurements of a Pt standard indicate that the accuracy of the magnetometer is better than 1%. The isothermal magnetic entropy change as a function of temperature was calculated from magnetization data using the Maxwell relation:

$$\Delta S_{\text{mag}}(T) = \int_0^{H_0} \left(\frac{\partial M}{\partial T} \right)_H dH. \quad (6)$$

III. SAMPLES

Four Gd samples were used in this study. Sample 1: a polycrystalline sample prepared commercially in Russia, grade Gd-M1. No detailed impurity content was supplied by the manufacturer, however, chemical analyses were made on this sample at the Materials Preparation Center (MPC) of the Ames Laboratory and the results are given in Table II along with the other three samples. Sample 2: a high-purity polycrystalline Gd sample prepared by the MPC, Ames Laboratory. Sample 3: a high-purity Gd single crystal prepared by the MPC, Ames Laboratory. Sample 4: a typical commercial standard purity polycrystalline sample from the Peoples' Republic of China. No detailed impurity content of sample 4 was supplied by the manufacturer, although the metal was claimed to be 99.9 wt. % pure. A chemical analysis, carried out on this specimen at the Ames Laboratory, showed that the claimed purity of 99.9 wt. % was approximately correct,

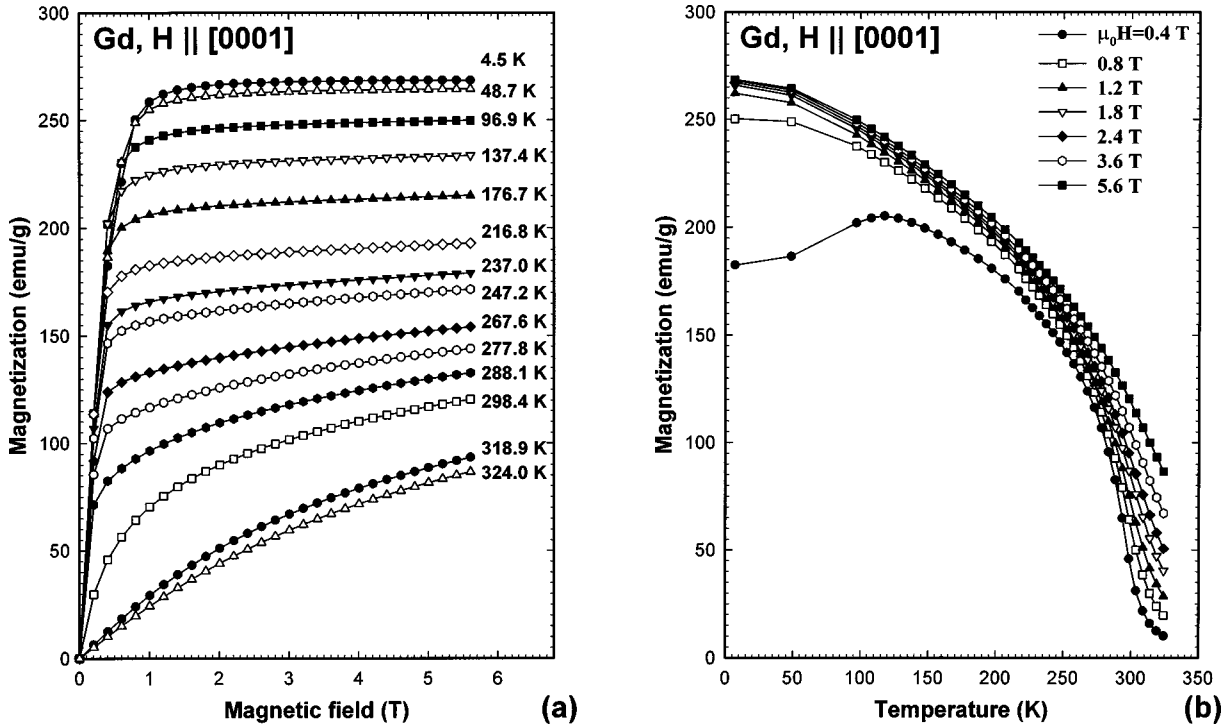


FIG. 1. Magnetization of a Gd single crystal as a function of field at selected temperatures (a), and the magnetization of Gd as a function of temperature at selected dc fields (b) with the field parallel to the [0001] direction.

but when one considers the purity on an atomic basis, it was only 93.1 at. % pure.

The specimens for the direct magnetocaloric effect (ΔT_{ad}) measurements were shaped as parallelepipeds having approximate dimensions $10 \times 4 \times 4 \text{ mm}^3$ which were cut in two pieces parallel to the longest dimension. The thermocouple was inserted between the two halves of such sliced parallelepipeds. The specimens for heat-capacity measurements were approximately cylindrically shaped and had a diameter of $\sim 10 \text{ mm}$ and a height of $\sim 3 \text{ mm}$. The samples for magnetization and susceptibility studies were in the form of parallelepipeds with the approximate dimensions $2 \times 2 \times 4 \text{ mm}^3$. All single-crystal Gd samples were cut from the same large single crystal after the crystallographic axes in the sample were located using back-reflection Laue photographs. The measurements on single-crystalline specimens were performed with the magnetic field parallel to the [0001] and $[10\bar{1}0]$ directions. The combined accuracy of the alignment of the crystallographic direction(s) with the direction of the magnetic field (cutting and positioning the specimens in the sample holders) was better than $\pm 5^\circ$.

IV. EXPERIMENTAL RESULTS

The magnetization of single-crystal Gd with the magnetic field applied parallel to the two different crystallographic directions is shown in Figs. 1 and 2. These data agree well with the results reported by Feron.²⁹ Gd is ferromagnetic in both directions with the [0001] direction being the easy axis of magnetization at high temperatures. The paraprocess field (the field at which the magnetization is approximately saturated) was found to be $\sim 0.8 \text{ T}$ parallel to the [0001] direction and $\sim 1.2 \text{ T}$ along the $[10\bar{1}0]$ direction at low temperatures. We were unable to detect any hysteresis in the

temperature and magnetic-field behavior of the magnetization of the Gd single crystals at any temperature. The experimental value of the saturation magnetization at 4.5 K is $7.63 \mu_B$ per Gd atom in either field direction which is almost 10% higher than the theoretically expected value of $gJ = 7.0 \mu_B$.

The ac susceptibility of the Gd single crystals in the two different directions is shown in Fig. 3. Its behavior is independent of the ac field frequency and the amplitude. The most distinct differences in the ac susceptibility behavior are observed in the region between T_{SR} and T_C , which can be explained by the rotation of easy magnetization axis. The small decrease in the susceptibility in both directions at low temperatures is probably due to the nonlinear dependence of the cone angle between the easy magnetization axis and the c axis of the crystal. The temperature dependence of the ac susceptibility with a bias dc field applied parallel to the [0001] direction is shown in Fig. 4, while Fig. 5 presents the same data with the dc field parallel to the $[10\bar{1}0]$ direction. These results are similar to those reported by Aliev, Kamilov, and Omarov.⁹ One can see that the Curie temperature increases with the increasing dc field and this tendency is maintained for both crystallographic directions.

The heat capacity was measured for three different samples (polycrystalline samples 2 and 4, and the single-crystal sample 3). The zero magnetic-field data are shown in Fig. 6 together with that reported by Griffel, Skochdopole, and Spedding.¹⁶ As can be seen, the heat capacity of both of the Ames Laboratory (MPC) samples (2 and 3), which are similar, with respect to the amount of impurities, agrees very well. The two curves are practically indistinguishable from ~ 3.5 to $\sim 350 \text{ K}$ except near the T_{SR} , see the following two paragraphs. The temperature and the height of the pro-

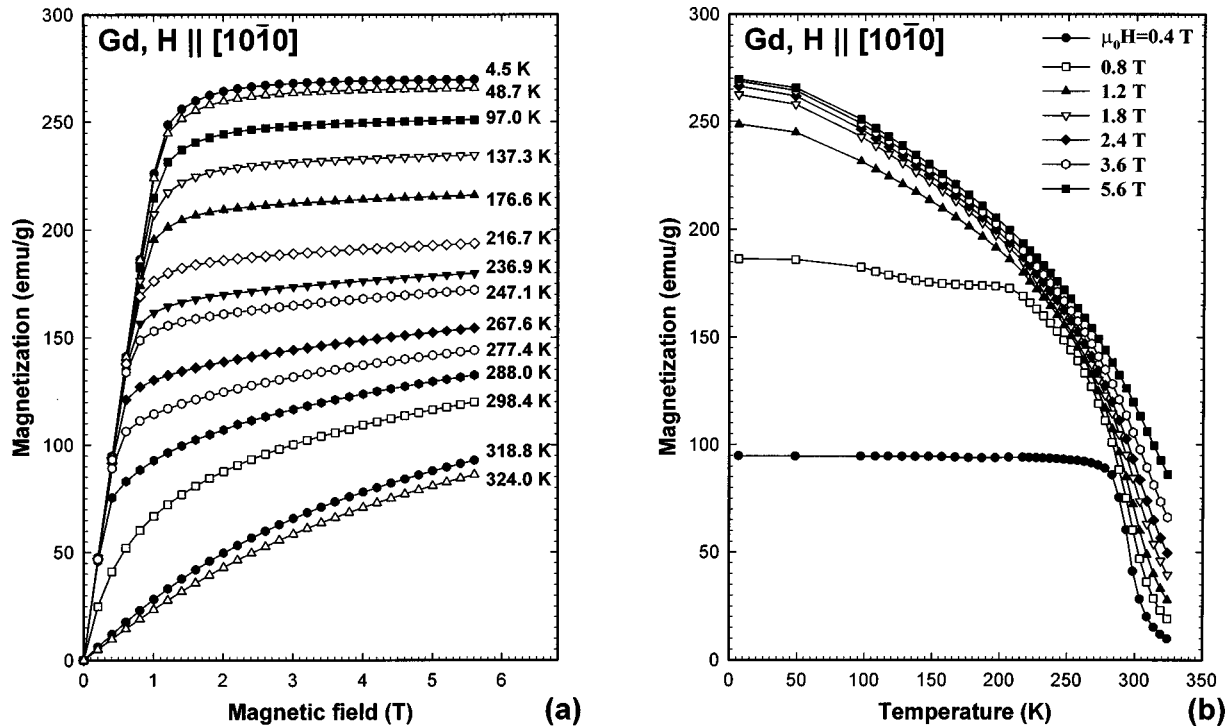


FIG. 2. Magnetization of a Gd single crystal as a function of field at selected temperatures (a), and the magnetization of Gd as a function of temperature at selected dc fields (b) with the field parallel to the $[10\bar{1}0]$ direction.

nounced λ -type anomaly which is observed near the Curie temperature are the same within the experimental accuracy indicating that both samples order at exactly the same temperature. A significant reduction of the purity of the sample (see the curve for sample 4) causes a distinct change in the behavior of the heat capacity. The maximum of the λ -type anomaly is sharply reduced in the magnitude ($\sim 10\%$) and

temperature ($\sim 5\%$). An excess heat capacity appears between ~ 70 and ~ 286 K and above ~ 300 K. This is most likely associated with the straining of the crystal lattice and the weakening of the exchange interactions by the large amount of interstitial impurities present in the sample (see Table II), which leads to a reduction of the Curie temperature

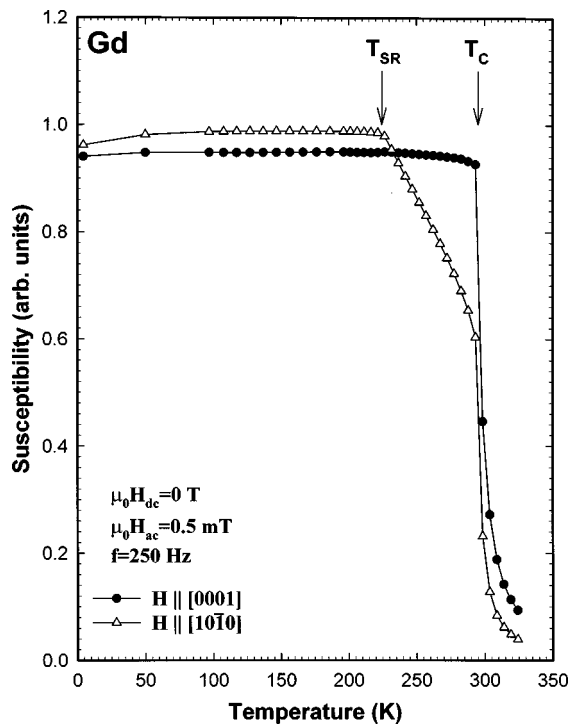


FIG. 3. The ac magnetic susceptibility of Gd single crystals with the ac field parallel to the $[0001]$ and $[10\bar{1}0]$ directions.

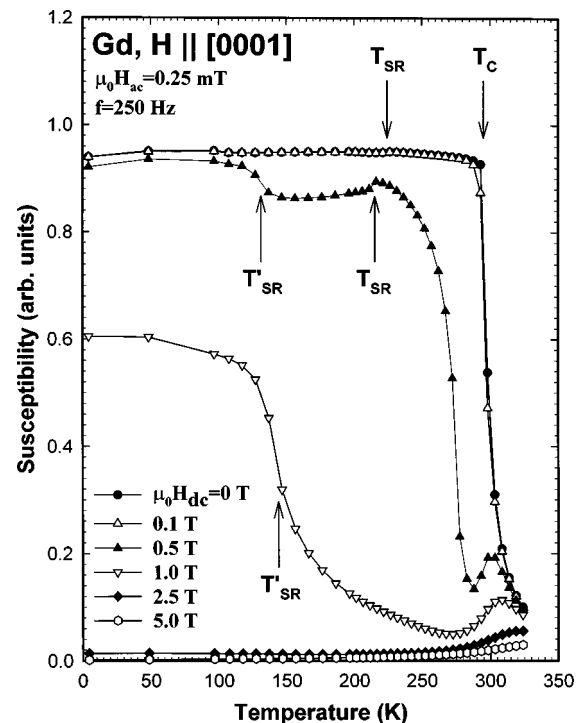


FIG. 4. The ac magnetic susceptibility of a Gd single crystal in bias dc fields with the ac and dc fields parallel to the $[0001]$ direction.

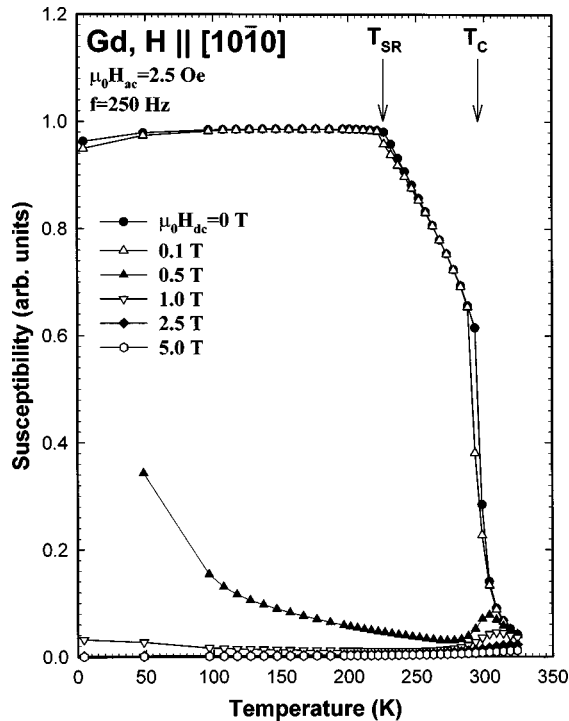


FIG. 5. The ac magnetic susceptibility of a Gd single crystal in bias dc fields with the ac and dc fields parallel to the $[10\bar{1}0]$ direction.

and to notably larger spin fluctuations both above and below the Curie temperature. It is not surprising that the heat capacity of the sample measured by Griffel, Skochdopole, and Spedding¹⁶ (also an Ames Laboratory sample prepared in 1953 by one of the authors of this paper, K.A.G., Jr.) generally falls between the two extreme cases (the clean Ames Laboratory samples and the impure commercial Gd). The heat capacity reported by these authors is closer to that of samples 2 and 3 since the purity (in at. %) of that specimen was much better than the purity of the commercial metal (sample 4), although it was lower than the purity of the two Ames Laboratory MPC's specimens used in this study. The major impurities in the metal used by Griffel *et al.* were Ta, Sm, and Y (the interstitial impurities were probably quite high, but at that time they were difficult to measure), while the major impurities in the commercial sample 4 were the interstitials (H, C, N, O, and F). The upturn in the heat capacity of the commercial Gd at low temperature (see the inset of Fig. 6) is associated with the high amount of oxygen impurity, and is due to the presence of $\text{Gd}_2\text{O}_{3-x}$ which orders magnetically at $\sim 2.6 \text{ K}$ or at $\sim 3.7 \text{ K}$ depending on the stoichiometry and the crystal structure of the oxide.³⁰

The magnetic heat capacity (in fields of 2, 5, 7.5, and 10 T) was measured on specimens 2, 3, and 4. The heat capacity of single-crystal samples was also measured with the magnetic field applied parallel to the $[0001]$ and $[10\bar{1}0]$ directions. Contrary to the distinct differences observed in magnetization and susceptibility, the differences between the heat capacity of single-crystal samples with magnetic field applied along the different crystallographic directions, if any, were smaller than the experimental errors. This may be partially due to the fact that the magnetocrystalline anisotropy in Gd is quite small, and that the lowest magnetic field used to

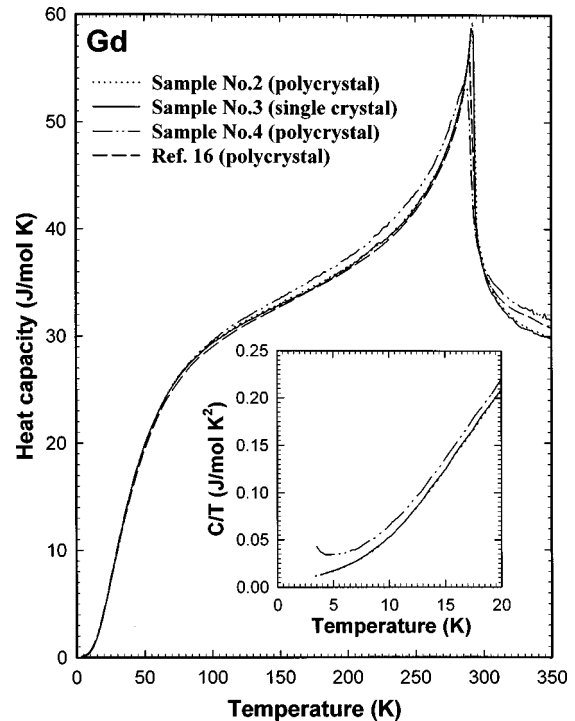


FIG. 6. The zero magnetic-field heat capacity of different Gd samples. The heat-capacity data have not been smoothed and are shown in a form of lines for clarity. The inset clarifies the low-temperature behavior as C/T vs T plot.

measure heat capacity (2 T) was already too large to reveal any possible differences in the magnetic heat capacity (note that the differences in magnetization and susceptibility also tend to disappear as magnetic field rises, see Figs. 1, 2, 4, and 5). A second reason is that the measured heat capacity is always a combined total of at least three contributions: electronic, lattice, and magnetic, and therefore, a relatively small difference due to the effect of the magnetic field on the magnetic entropy when applied in different crystallographic directions would be practically invisible when overlapped with the much larger field-independent lattice heat capacity.

Figure 7 displays the heat capacity of the Gd single crystal in magnetic fields up to 10 T applied parallel to the $[0001]$ direction. The magnetic field has a pronounced effect on the λ -type maximum: it is considerably broadened and is shifted to higher temperatures as the magnetic field increases. This behavior is typical for ferromagnetic materials. The sample purity has practically the same effect on the magnetic heat capacity as on the zero-field heat capacity (see Fig. 6). A small heat-capacity anomaly exists in the zero magnetic-field data near $\sim 220\text{--}225 \text{ K}$, but it is wiped out by magnetic fields as low as 2 T (see the inset of Fig. 7). It is only observed in the heat capacity of the two single-crystal samples and it is indistinct in the heat capacity of the Ames Laboratory polycrystalline Gd sample 2, even though the latter has lower overall and interstitial impurity contents than the single crystal.

The adiabatic temperature change (i.e., the magnetocaloric effect, MCE) was measured on three different samples, 1, 2, and 4. The low-field (0–2 T) results for sample 2 in quasistatic and pulse magnetic fields are shown in Fig. 8 together with the MCE calculated from the magnetic heat-

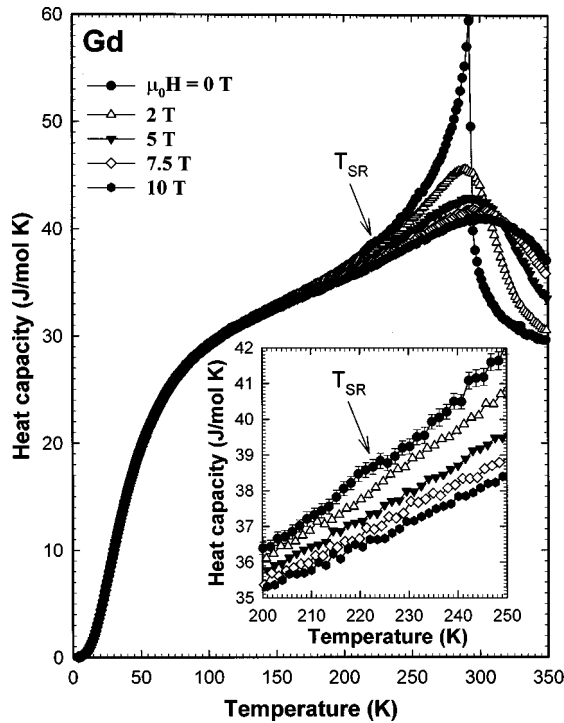


FIG. 7. The heat capacity of single-crystal Gd with the magnetic field applied parallel to the [0001] direction. The inset clarifies the details near the spin reorientation transition T_{SR} . The error bars are shown for the zero-field heat capacity in the inset. The arrows point to the anomaly at T_{SR} .

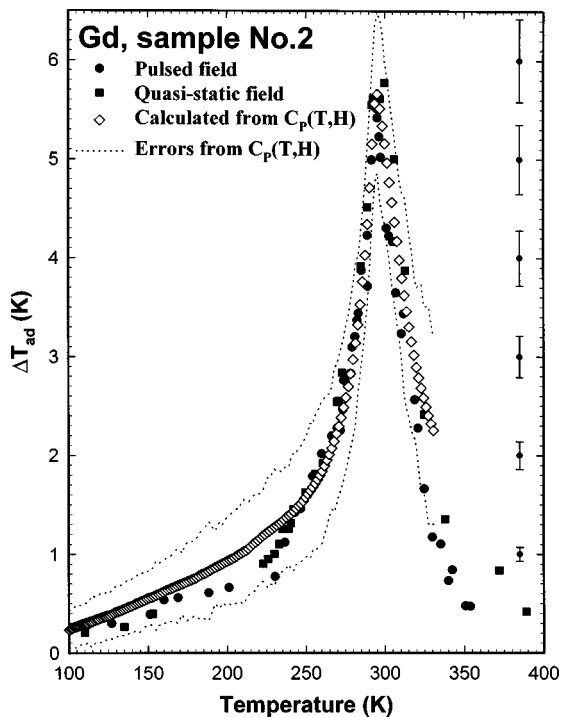


FIG. 8. The magnetocaloric effect in Gd measured directly in quasistatic and pulsed fields (filled symbols) compared with that calculated from the heat capacity (opened symbols) for a magnetic field change from 0 to 2 T. The error bars on the right-hand side of the figure indicate the uncertainty in the direct measurements ($\pm 7\%$).

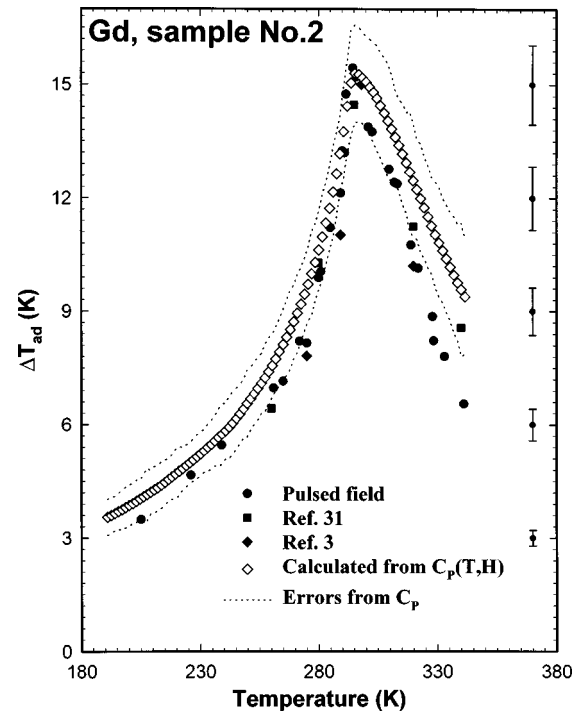


FIG. 9. The magnetocaloric effect in Gd measured directly in a pulsed field compared with that calculated from the heat capacity for a magnetic field change from 0 to 7.5 T. Results from Refs. 3 and 31 were obtained on samples of different purities and are shown for comparison. The error bars on the right-hand side of the figure indicate the uncertainty in the direct measurements ($\pm 7\%$).

capacity measurements. The best agreement between the results obtained using three different techniques is observed in the temperature range from ~ 220 to ~ 330 K. However, the direct MCE results agree quite well with MCE values calculated from the heat capacity when considering the error limits of both measurements even outside this temperature range. The maximum ΔT_{ad} of ~ 5.8 K is observed at ~ 295 K which is close to the Gd Curie temperature. The magnetocaloric effect for a larger magnetic field change (from 0 to 7.5 T) is shown in Fig. 9 for the same sample (2) together with several data sets reported in the literature for the same magnetic field change for different Gd samples. The agreement is again quite good, well within the experimental error limits of the two techniques, and the maximum MCE of ~ 15 K also occurs at ~ 295 K. The magnetocaloric effect rises as the magnetic-field change increases. The MCE rise is, however, a nonlinear function of the magnetic field which is illustrated in Fig. 10 where the field dependence of the maximum of the MCE, which occurs close to the Curie temperature, is shown. At lower magnetic fields the specific magnetocaloric effect rate change at $T \cong T_C$ is close to 3 K/T, and it is reduced to ~ 2.2 K/T at 5 T and to ~ 1.8 K/T at 10 T.

Figure 11 illustrates the effect of impurities on the magnetocaloric effect in Gd. The MCE measured directly on the high-purity sample from Ames Laboratory (2) is approximately equal to that of the sample prepared in Russia (1). Both the temperature of the MCE peak and its behavior as a function of temperature are similar for those two samples. The MCE of the commercial purity Gd (sample 4) is dis-

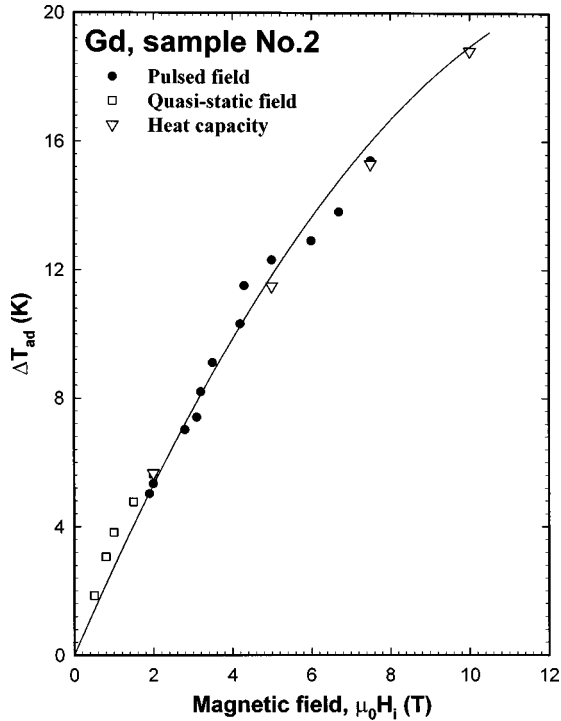


FIG. 10. The magnetocaloric effect at $T \cong T_C$ for polycrystalline Gd as a function of the magnetic field change from 0 to H_i .

tinctly lower, well outside the experimental error. The lowering of the MCE peak temperature was expected from the heat-capacity results (e.g., see Fig. 6), but the reduction of ΔT_{ad} is surprisingly rather large. This is particularly puzzling when one compares the MCE's calculated from the heat capacity for samples 2 and 4, which are quite close, within experimental error, see Fig. 11. This is also puzzling from the fact that sample 1 is slightly more impure than sample 4, but its ΔT_{ad} is in good agreement with the pulse field and heat-capacity values for the high-purity Gd sample (2). Examination of the impurity contents reveals that the oxygen is ~ 3 times larger in sample 1 than in sample 4, while the carbon content is ~ 4 times, and the fluorine content is ~ 60 times larger in sample 4 than in sample 1. It is obvious that O does not cause this diminution in ΔT_{ad} , but either C or F is the culprit. Both O and F are present as compounds, Gd_2O_{3-x} and GdF_3 in the Gd metal matrix segregating on grain boundaries, but C is known to dissolve in Gd. We believe that the dissolved interstitial carbon has a strong influence on the results obtained in a dynamic pulsed field (i.e., direct MCE measurements) as compared to the static field (heat-capacity) measurements. As already noted above, the interstitials not only interfere with the exchange interaction, but they also strain the crystal lattice significantly. It is quite possible that a strained lattice complicates the coupling of magnetic atoms with the magnetic field, and this is particularly critical for the short duration of the pulse, ~ 0.2 s (Ref. 26) (and obviously the maximum field values last just a fraction of this time). Therefore, this short time period is sufficient to induce a full response of the nonstrained lattice of magnetic ions, and thus measures the MCE correctly in pure materials. However, the pulse time is probably too short for an adequate response of the magnetic atoms to yield the correct MCE in strained lattices which contain a large amount

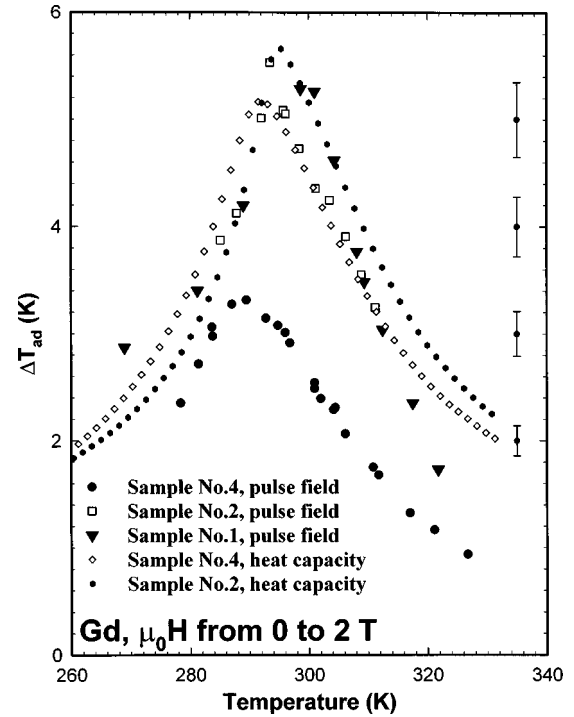


FIG. 11. The magnetocaloric effect as a function of temperature measured in a pulsed magnetic field from 0 to 2 T for three different samples. The error bars on the right-hand side of the figure indicate the uncertainty in the pulsed field measurements ($\pm 7\%$).

of dissolved interstitial impurities. This result correlates well with an earlier study of the effect of a controlled amount of carbon in polycrystalline Gd,³² where the authors showed that randomly distributed interstitial carbon significantly changes the magnetothermal properties of the metal.

V. DISCUSSION

A. Paramagnetic \leftrightarrow ferromagnetic phase transition

First we will discuss the question about the determination of the exact Curie temperature of Gd. Besides the confirming the fact^{10,32} that the ordering temperature depends on the amount of impurities in the metal (see Fig. 6), it is also important to examine the effect of how the different experimental data are analyzed, which may have an effect on the final result with regard to the value of the Curie temperature. The results of different approaches to determining the Curie temperature for the two single-crystal samples along both crystallographic directions based on different experimental techniques utilized in this work are listed in Table III.

It is well known that the Curie temperature in zero magnetic field is rigorously defined as a temperature where the spontaneous magnetization, and hence, the magnetic order parameter η experiences the fastest change as a function of temperature. Then, if one can measure magnetic susceptibility or magnetization in zero magnetic field, the temperature where susceptibility or magnetization increases (decreases) most rapidly would be an adequate representation of the Curie point. Usually if any property P varies as a function of temperature, then the location of the inflection point (i.e., where $\partial^2 P / \partial T^2 = 0$) corresponds to the fastest change of a given property with the temperature and determines the

TABLE III. The paramagnetic \leftrightarrow ferromagnetic ordering temperature (estimated standard deviation in the last significant digit is given in parentheses) of single-crystal Gd as determined from different experimental data.

	$\mu_0H=0$ T		$\mu_0H=2$ T		$\mu_0H=5$ T		$\mu_0H=7.5$ T		$\mu_0H=10$ T	
	$\parallel c$	$\parallel a$	$\parallel c$	$\parallel a$	$\parallel c$	$\parallel a$	$\parallel c$	$\parallel a$	$\parallel c$	$\parallel a$
ac magnetic susceptibility	293(2)	293(2)								
Magnetization	297(2) (0.2 T)	296(2) (0.2 T)	306(3)	307(3)	322(5)	324(5)				
MCE ^a (maximum)	294(1)	295(1)	310(1)	310(1)	326(3)		336(3)			
Heat capacity ^b (maximum)	291(1)	291(1)	290(1)	290(1)	292(1)	293(1)	295(2)		302(3)	
Heat capacity (inflection)	294(1)	294(1)	310(1)	309(1)	329(2)	327(3)	341(3)			
Thermodynamic method (Arrot plot)	295(1)	295(1)								

^aThe ordering temperatures listed in this row are determined from the maximum magnetocaloric effect observed when magnetic field was changed from 0 to $\mu_0H=2$ T (column $\mu_0H=0$ T), from 2 to 5 T (column $\mu_0H=2$ T), from 5 to 7.5 T (column $\mu_0H=5$ T), and from 7.5 to 10 T (column $\mu_0H=7.5$ T).

^bThe heat capacity with the magnetic field parallel to the a axis was not measured in magnetic fields higher than 5 T because the sample in the calorimeter was twisted by fields higher than 5 T.

phase-transition temperature, provided all other thermodynamic parameters are kept constant. This approach could be used to determine ordering temperature in a nonzero magnetic field, in which case position of the inflection point corresponds to the temperature of the fastest transformation of magnetic structure and/or transition between short- and long-range magnetic order. Since the ac susceptibility was measured in low ac fields (0.25 to 1.0 mT), then it is possible to assume that such a low magnetic field does not affect the magnetic order parameter and thus, T_C from the ac susceptibility (Table III) calculated as the temperature of the inflection point represents the Curie temperature in zero magnetic field. The same technique was used to determine the ferromagnetic ordering temperature from magnetization measurements in essentially nonzero magnetic fields, the second row in Table III. Note, that since the T_C from the magnetization was calculated from the experimental data measured in 0.2 T field, then the result should not be directly compared with that obtained in zero field. Next, as discussed in the Introduction, the MCE is maximum at or close to the appropriate magnetic phase-transition temperature of the magnetic material because this maximum corresponds to the fastest change of the material's temperature as a function of field. Thus, the next row in the Table III shows the Curie temperature determined as the temperature where the maximum MCE occurs. The MCE maximum for nonzero magnetic fields (i.e., the ordering temperatures in nonzero magnetic fields) was determined as the point where MCE peak is observed for magnetic field change from H_1 to H_2 . Here H_1 is the lower field and H_2 is the upper field. Hence, for the column displaying the ordering temperature at $\mu_0H=2$ T the lower field is 2 T, etc. The next row displays the temperature where the heat-capacity maximum in different magnetic fields occurs. It has been suggested by Schmitt and co-workers,^{13,14} that the magnetic ordering temperature is most adequately represented by

the temperature where the heat capacity changes most rapidly, i.e., by the temperature of the heat-capacity inflection point above the heat-capacity maximum. Therefore, the appropriate calculation results are listed in the row entitled "Heat capacity (inflection)." Finally, the last row lists the thermodynamic Curie temperature in zero magnetic field which was determined using magnetization data by the thermodynamic method from Arrot plots.³³ The paramagnetic-to-ferromagnetic magnetic ordering temperature at high magnetic fields was determined in the same manner as in zero field—the inflection points for magnetization and heat capacity, and the maximum for the MCE. For the purposes of this paper we will still call this point the Curie temperature. The ac susceptibility in bias dc magnetic field 2 T was not measured. Since the upper temperature limit of our magnetometer was not high enough to estimate the Curie temperature from the ac susceptibility in magnetic fields >2 T (see Figs. 4 and 5), the appropriate data are not listed in Table III.

The first conclusion which is immediately obvious from an analysis of the data listed in Table III is that the temperature of the heat-capacity maximum does not correspond to the magnetic ordering temperature and it is always lower than the actual T_C . To the contrary, the heat-capacity inflection point and those determined from different experimental data (other than the magnetization data taken at 0.2 T) agree quite well, within ± 1 K. Hence, within the accuracy of experiment the ferromagnetic ordering in single-crystal Gd with overall purity listed in Table II occurs at the same Curie temperature, $T_C=294(1)$ K, in zero magnetic field. As the magnetic field rises, the ferromagnetic ordering in Gd occurs at a higher temperature. Single-crystal Gd orders at 297(2) K at 0.2 T; 309(2) K at 2 T; 326(4) K at 5 T, and 339(5) K at 7.5 T independent of the single-crystal orientation in the magnetic field. The field dependence of the ordering tem-

perature is close to linear in magnetic fields between 2 and 7.5 T with the slope of ~ 6 K/T, but has a higher slope below 2 T. This increase in the ferromagnetic ordering temperature of Gd with increasing dc field is expected since a strong magnetic field should assist the alignment of the magnetic moments. The fact that there is no apparent difference between the ordering temperature when the single crystal changes its orientation with regard to the direction of the field is indicative of the easy rotation of magnetic domains in the studied specimens, which is consistent with the high purity of Gd, and the small magnitude of the magnetic anisotropy energy.

B. The spin reorientation transition and ac susceptibility

An analysis of the behavior of the ac magnetic susceptibility along the $[10\bar{1}0]$ direction (Fig. 3) and the heat capacity in zero magnetic field (Fig. 7) suggests that the temperature of the spin reorientation transition is 227(2) K, which is close to the reported value of 230 K.² Our experimental data, unfortunately, do not permit us to make a conclusion about the exact effect of the dc magnetic field on the spin reorientation transition. Nonetheless, as can be seen in Figs. 4 and 5, a dc magnetic field has a different effect on a susceptibility anomaly associated with spin reorientation depending on the orientation of the magnetic field. First, the T_{SR} , where the easy magnetization axis starts to depart from the $[0001]$ direction, seems to be suppressed from 227 K down to $\sim 214(3)$ K by 0.5 T dc field applied parallel to the $[0001]$ direction and the corresponding anomaly becomes indistinguishable when the field is either less than 0.5 or increases to 1 T. Second, it is known² that in zero field the cone angle between the $[0001]$ direction and easy magnetization axis decreases nonlinearly as the temperature decreases starting from ~ 180 K. Hence, the low-temperature anomaly (at ~ 132 K) in the ac susceptibility in a 0.5 T bias dc field, Fig. 4, is probably indicative of the change of the easy magnetization axis by an increasing magnetic field. This is also supported by the fact that the higher dc field of 1 T shifts this low-temperature anomaly from 132(2) to 142(3) K (the temperatures are determined from the corresponding inflection points). As mentioned above, the higher dc magnetic fields (2 T from heat capacity, and 2.5 T from ac susceptibility) eradicate the differences between the behavior of Gd in different crystallographic directions. This suggests that at magnetic fields higher than 2–2.5 T Gd remains ferromagnetic from the Curie temperature down to at least 4.2 K without changing the easy magnetization axis, i.e., the spin reorientation transition switching the easy magnetization axis from the $[0001]$ to the $[10\bar{1}0]$ is completely quenched by magnetic fields larger than 2–2.5 T.

The ac susceptibility anomaly which occurs at ~ 132 K in 0.5 T magnetic field (Fig. 4) closely resembles that observed earlier in zero-field dc susceptibility (see Fig. 2.1 from Ref. 3). That is, the anomaly disappears as the dc field increases, which is consistent with our results. The abnormal behavior of Young's modulus in zero field³⁴ and other properties of single-crystalline Gd in the vicinity of this temperature have also been observed.³ Tishin and Martynenko³ have suggested that this behavior is associated with the existence of a local minimum of magnetic anisotropy energy which can lead to

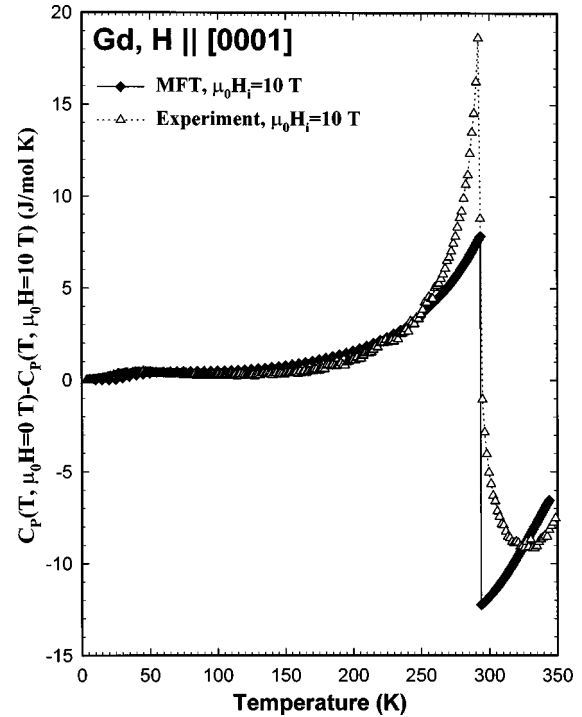


FIG. 12. The effect of the magnetic field on the change of the heat capacity of single crystal Gd in a field of 10 T relative to zero field as compared to the theoretically predicted values from mean-field theory (MFT) for a field 10 T.

an anomalous dependence of the angle between the $[0001]$ direction and the magnetic moment.

Increasing the bias dc magnetic field causes the development of a distinct maximum (at ~ 300 K) in the behavior of the ac susceptibility (Figs. 4 and 5) which is apparently associated with the ferromagnetic \leftrightarrow paramagnetic transition, since it is shifted to higher temperatures as the field increases. However, since the temperature of the maximum is notably higher (by ~ 20 K) than the ordering temperature determined from the other experimental data (see previous section and Table III), then it is most likely due to changes in the short-range magnetic order just above the magnetic phase transition. The rapid rise of the ac susceptibility along $[0001]$ direction, Fig. 4, in the 0.5 T dc field just below T_C is quite different from the ac susceptibility along $[10\bar{1}0]$, Fig. 5, in the same dc field of 0.5 T. Correspondingly, we see a large difference in the ac susceptibilities along the two directions for the data measured at a 1 T dc bias field. But at 2.5 T the temperature dependences of the ac susceptibilities are once again similar for the two orientations. The origin of this difference is not completely understood without the availability of direct studies of the magnetic structure.

C. Magnetic heat capacity

Assuming that the dc magnetic field affects only the magnetic part of the heat capacity C_{mag} , one can compare the experimentally observed effect with that calculated theoretically from molecular field theory.³ The results are displayed in Fig. 12 in the form of the difference between experimental heat capacity at zero magnetic field and that at 10 T together with the theoretically predicted ΔC_{mag} from the mean-field

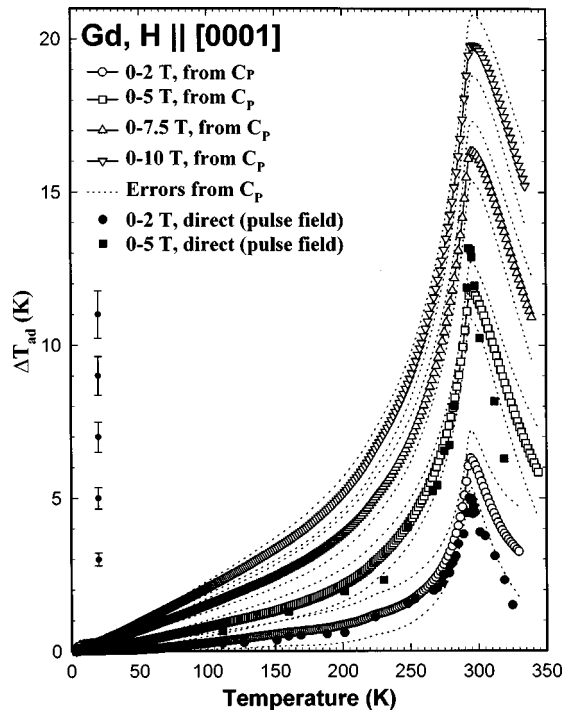


FIG. 13. The magnetocaloric effect in single crystal Gd with the magnetic field applied parallel to the [0001] direction. The error bars on the left-hand side of the figure indicate the uncertainty in the direct measurements ($\pm 7\%$).

theory for a magnetic field 10 T. As is obvious from Fig. 12, the agreement is quite good at temperatures well below and well above ($> \pm 25$ K) the paramagnetic \leftrightarrow ferromagnetic phase transition in zero field, and near the phase transition there is a qualitative agreement between experiment and theory. Furthermore, the theoretical prediction does not account for the small anomaly due to spin reorientation transition at ~ 227 K.

D. Magnetocaloric effect

Experimental measurements of the MCE using different techniques revealed that within the experimental accuracy it is independent of the crystal orientation in magnetic fields stronger than 2 T. The adiabatic temperature rise in the Gd single crystal with the magnetic field applied parallel to the [0001] is shown in Fig. 13. The open symbols represent ΔT_{ad} as calculated from magnetic heat-capacity data for a field change 0–2, 0–5, 0–7.5, and 0–10 T and the filled symbols represent that measured directly in pulse fields 0–2 and 0–5 T. The dotted lines in Fig. 13 delineate the range of estimated errors in ΔT_{ad} as determined from heat capacity using Eq. (5), and the error bars on the left side of the figure indicate the error limits in the direct measurements. The adiabatic temperature change in single-crystal Gd compares well with that measured on our polycrystalline samples and that reported by other groups.^{35–38}

As noted above, the MCE calculated from heat capacity agrees quite well with that measured directly in pulse fields, especially when considering the uncertainties of the two techniques. However, if one ignores the error limits of the two measurements, a consistent behavior is observed: the directly measured values lie below the heat-capacity data re-

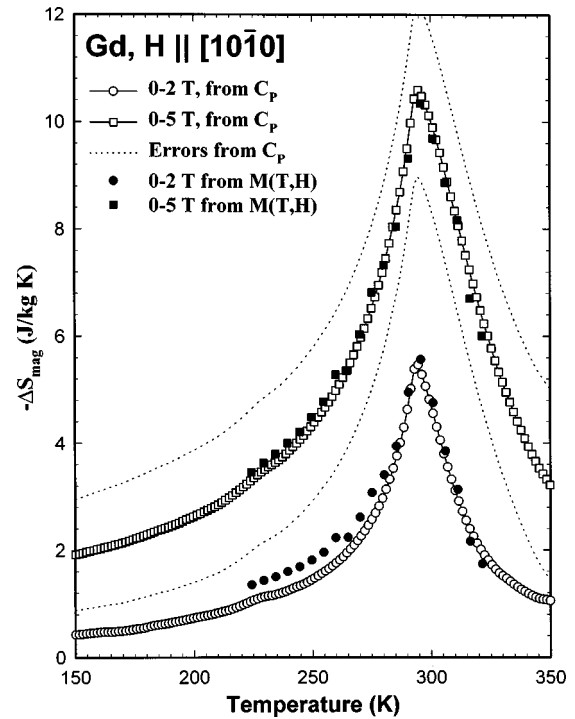


FIG. 14. The magnetic entropy change in single crystal Gd with the magnetic field applied parallel to the [1010] direction as determined from heat-capacity and magnetization measurements.

sults at the highest temperatures (see Figs. 8, 9, and 13). The most likely reasons which can account for this difference are as follows. First, as can be seen from Eq. (5), the experimental errors in ΔT_{ad} calculated from heat capacity are directly proportional to the errors in the total entropy [i.e., to the experimental errors in heat capacity, Eqs. (5) and (3)], and they are inversely proportional to the slope of $S(T, H_i)$ curve as a function of temperature. It should be noted, that the experimental errors in $C_p(T, H)$ do not change radically at higher temperatures, i.e., they remain at the same $\sim 0.5\%$ level. Accordingly, there is no sharp increase of the errors in total entropy. However, the slope of $S(T, H_i)$ is significantly lower above the Curie temperature, i.e., when the heat capacity reaches its maximum and starts to decrease [see Eqs. (1) and (2), and Figs. 6 and 7, and noting that $dS/dT = C/T$]. Indeed, this slope reduction lowers the dS/dT terms in Eq. (5) and rises the overall $\sigma\Delta T$. Therefore, the experimental errors in $\Delta T_{ad}(T)$ become inherently larger immediately above the Curie temperature where the slope of $S(T, H_i)$ curve decreases.

Second, since the measurement time in the pulse-field technique for the direct measurements of ΔT_{ad} is quite short (~ 0.2 s), the samples are not thermally insulated.²⁶ However, the thermal conductivity of Gd is larger in the paramagnetic state compared to that in the ferromagnetic state. Therefore, this increase in thermal conductivity may lead to larger thermal losses above the Curie temperature due to the heat exchange with the surrounding air and radiation losses, thus lowering the observed ΔT_{ad} value.

The isothermal magnetic entropy change in Gd with the magnetic field parallel to the [1010] direction is shown in Fig. 14. As with the adiabatic temperature rise, the $\Delta S_{mag}(T)$ is close to that measured earlier on polycrystalline samples

of different purity.^{8,15,37–39} The $\Delta S_{\text{mag}}(T)$ values were calculated from heat-capacity data (open symbols) as the isothermal difference between $S(T, H=0)$ and $S(T, H_i)$ for H_i equal to 2 and 5 T. The dotted lines represent margins of experimental errors in ΔS_{mag} from the heat-capacity data [Eq. (4)] for magnetic field change 0 to 5 T. Unlike the ΔT_{ad} , the errors calculated from the heat capacity for ΔS_{mag} do not rise when temperature exceeds the Curie temperature and the error $\sigma \Delta S_{\text{mag}}$ remains approximately the same for any magnetic field change. The results from magnetization data (filled symbols) were obtained by numerical integration, Eq. (6). The excellent agreement between the results obtained from magnetization and from heat-capacity measurements is obvious.

VI. CONCLUSIONS

As a result of experimental studies of the magnetic and thermal properties of four different samples of Gd we confirm that purity plays an important role in obtaining the intrinsic properties. The large amount of impurities typically found in commercially designated “99.9 wt. % purity” Gd, lowers the Curie temperature and also broadens the temperature range of the paramagnetic↔ferromagnetic transition, while masking the spin reorientation transition which is obvious in much higher-quality single-crystalline samples. By combining the results from magnetization, ac susceptibility, heat-capacity, and direct magnetocaloric effect measure-

ments, we found that in zero magnetic field the Curie temperature of Gd equals 294(1) K and that the spin reorientation temperature is 227(2) K. We found that between 2 and 7.5 T, T_C in Gd increases by ~ 6 K/T, with the increase of the T_C with the magnetic field being approximately linear. The spin reorientation transition appears to be quenched entirely by magnetic fields higher than 2–2.5 T. This study is an attempt to evaluate the magnetocaloric properties of pure Gd utilizing four different techniques on the same samples: direct measurements of the adiabatic temperature rise in quasistatic and pulsed magnetic fields, heat-capacity, and magnetization measurements. In general, the MCE properties were found to be essentially identical and independent of the experimental technique used. The one notable exception was a Gd sample which contained a large amount of interstitial impurities when the direct measurements were made using pulsed magnetic fields. It is believed that the dissolved impurities strain the lattice and the magnetic atoms cannot fully respond to the rapidly changing field.

ACKNOWLEDGMENTS

This work was supported in part by the Office of Basic Energy Sciences Materials Sciences Division, U.S. Department of Energy, under Contract No. W-7405-ENG-2 (V.K.P. and K.A.G.), and by NATO Linkage Grant No. 950700 (all authors).

*Author to whom correspondence should be addressed: Vitalij K. Pecharsky, 242 Spedding, Ames Laboratory, Iowa State University, Ames, IA 50011-3020; Fax: (515)-294-9579; Electronic address: Vitkp@AmesLab.Gov

¹K. A. McEwen, in *Handbook on the Physics and Chemistry of Rare Earths*, edited by K. A. Gschneidner, Jr. and Le Roy Eyring (North-Holland, Amsterdam, 1978), Vol. 1, p. 411.

²J. M. Cable and L. O. Wollan, *Phys. Rev.* **165**, 733 (1968).

³A. M. Tishin and O. P. Martynenko, *Physics of Rare Earth Metals in the Vicinity of Magnetic Phase Transitions* (Nauka, Moscow, 1995).

⁴S. Yu. Dan'kov, T. I. Ivanova, and A. M. Tishin, *Sov. Tech. Phys. Lett.* **18**, 254 (1992).

⁵Kh. K. Aliev, I. K. Kamilov, and A. M. Omarov, *Sov. Phys. JETP* **67**, 2262 (1988).

⁶D. J. W. Geldart, P. Howgraves, N. M. Fujiki, and R. A. Dunlap, *Phys. Rev. Lett.* **62**, 2728 (1989).

⁷H. E. Nigh, S. Legvold, and F. H. Spedding, *Phys. Rev.* **132**, 1092 (1963).

⁸B. K. Ponomarev, *J. Magn. Magn. Mater.* **61**, 129 (1986).

⁹Kh. K. Aliev, I. K. Kamilov, and A. M. Omarov, *Sov. Phys. Solid State* **26**, 508 (1984).

¹⁰K. A. Gschneidner, Jr., *J. Alloys Compd.* **193**, 1 (1993).

¹¹W. D. Corner, W. C. Roe, and K. N. R. Taylor, *J. Phys. Soc. Jpn.* **17**, 1310 (1962).

¹²E. S. R. Gopal, *Specific Heats at Low Temperatures* (Plenum, New York, 1966).

¹³J. A. Blanco, D. Gignoux, and D. Schmitt, *Phys. Rev. B* **43**, 13 145 (1991).

¹⁴M. Bouvier, P. Lethillier, and D. Schmitt, *Phys. Rev. B* **43**, 13 137 (1991).

¹⁵V. K. Pecharsky and K. A. Gschneidner, Jr., *Adv. Cryog. Eng.* **42A**, 423 (1996).

¹⁶M. Griffel, R. E. Skochdopole, and F. H. Spedding, *Phys. Rev.* **93**, 657 (1954).

¹⁷P. C. Lanchester, K. Robinson, D. P. Baker, I. S. Williams, R. Street, and E. S. R. Gopal, *J. Magn. Magn. Mater.* **15-18**, 461 (1980).

¹⁸G. Glorieux, J. Thoen, G. Bednarz, M. A. White, and D. J. W. Geldart, *Phys. Rev. B* **52**, 12 770 (1995).

¹⁹F. J. Darnell and W. H. Cloud, *J. Appl. Phys.* **35**, 935 (1964).

²⁰S. Legvold, F. H. Spedding, F. Barson, and J. F. Elliot, *Rev. Mod. Phys.* **25**, 129 (1953).

²¹T. J. McKenna, S. J. Campbell, D. H. Chaplin, and G. V. H. Wilson, *J. Magn. Magn. Mater.* **20**, 207 (1980).

²²H. R. Child, *Phys. Rev. B* **18**, 1247 (1978).

²³A. Vaterlans, T. Beutler, and F. Meier, *Phys. Rev. Lett.* **67**, 3314 (1991).

²⁴C. Glorieux, J. Caerels, and J. Thoen, *J. Appl. Phys.* **80**, 3412 (1996).

²⁵G. V. Brown, *J. Appl. Phys.* **47**, 3673 (1976).

²⁶S. Yu. Dan'kov, A. M. Tishin, V. K. Pecharsky, and K. A. Gschneidner, Jr., *Rev. Sci. Instrum.* **68**, 2432 (1997).

²⁷V. K. Pecharsky, J. O. Moorman, and K. A. Gschneidner, Jr., *Rev. Sci. Instrum.* **68**, 4196 (1997).

²⁸R. W. Hill, S. J. Collocott, K. A. Gschneidner, Jr., and F. A. Schmidt, *J. Phys. F* **17**, 1867 (1987).

²⁹J. L. Feron, Ph.D. thesis, Grenoble, 1969.

³⁰A. E. Miller, F. J. Jelinek, K. A. Gschneidner, Jr., and B. C. Gerstein, *J. Chem. Phys.* **55**, 2647 (1971).

³¹B. K. Ponomarev, *Instrum. Exp. Tech.* **26**, 659 (1983).

- ³²L. B. Robinson and F. Milstein, *Solid State Commun.* **13**, 97 (1973).
- ³³A. Arrot, *Phys. Rev.* **108**, 1394 (1957).
- ³⁴Yu. I. Spichkin, A. M. Tishin, and K. A. Gschneidner, Jr. (unpublished).
- ³⁵T. Hashimoto, T. Numusawa, M. Shino, and T. Okada, *Cryogenics* **21**, 647 (1981).
- ³⁶B. R. Gopal, R. Chahine, and T. K. Bose, *Rev. Sci. Instrum.* **68**, 1818 (1997).
- ³⁷M. Földeàki, R. Chahine, and T. K. Bose, *J. Appl. Phys.* **77**, 3528 (1995).
- ³⁸A. M. Tishin, *Cryogenics* **30**, 127 (1990).
- ³⁹M. D. Kuzmin and A. M. Tishin, *Cryogenics* **33**, 868 (1993).